PHYTOTHERAPY RESEARCH
Phytother. Res. (2016)
Published online in Wiley Online Library
(wileyonlinelibrary.com) **DOI**: 10.1002/ptr.5615

Polyphenol-Rich Fraction from *Larrea divaricata* and its Main Flavonoid Quercetin-3-Methyl Ether Induce Apoptosis in Lymphoma Cells Through Nitrosative Stress

Renzo Martino,[1]* María Laura Barreiro Arcos,[2] Rosario Alonso,[1] Valeria Sülsen,[1] Graciela Cremaschi[2] and Claudia Anesini[1]

[1]Instituto de Química y Metabolismo del Fármaco — IQUIMEFA (UBA-CONICET), Facultad de Farmacia y Bioquímica, Universidad de Buenos Aires, Junín 956 piso 2, 1113, Ciudad Autónoma de Buenos Aires, Buenos Aires, Argentina
[2]Instituto de Investigaciones Biomédicas (BIOMED), Consejo Nacional de Investigaciones Científicas y Técnicas (CONICET), Facultad de Ciencias Médicas, Pontificia Universidad Católica Argentina (UCA), Av. A. Moreau de Justo 1600, piso 3, 1107AFF, Buenos Aires, Argentina

Larrea divaricata **is a plant with antiproliferative principles. We have previously identified the flavonoid quercetin-3-methyl ether (Q-3-ME) in an ethyl acetate fraction (EA). Both the extract and Q-3-ME were found to be effective against the EL-4 T lymphoma cell line. However, the mechanism underlying the inhibition of tumor cell proliferation remains to be elucidated. In this work, we analyzed the role of nitric oxide (NO) in the induction of apoptosis mediated by Q-3-ME and EA. Both treatments were able to induce apoptosis in a concentration-dependent and time-dependent manner. The western blot analysis revealed a sequential activation of caspases-9 and 3, followed by poly-(ADP-ribose)-polymerase cleavage. EA and Q-3-ME lowered the mitochondrial membrane potential, showing the activation of the intrinsic pathway of apoptosis. Q-3-ME and EA increased NO production and inducible NO synthase expression in tumor cells. The involvement of NO in cell death was confirmed by the nitric oxide synthases inhibitor L-NAME. In addition, EA and Q-3-ME induced a cell cycle arrest in G0/G1 phase. These drugs did not affect normal cell viability. This data suggested that EA and Q-3-ME induce an increase in NO production that would lead to the cell cycle arrest and the activation of the intrinsic pathway of apoptosis.**

Keywords: Larrea divaricata; ethyl acetate fraction; quercetin-3-methyl ether; T lymphoma cells; nitric oxide; apoptosis.

INTRODUCTION

Cancer is the leading cause of death worldwide, and according to the World Health Organization, this disease produced 8.2 million deaths in 2012 (Ferlay *et al*., 2015). Among cancers, leukemia and lymphoma are a group of heterogeneous neoplastic disorders of white blood cells characterized by the uncontrolled proliferation and the blockage in the differentiation process of hematopoietic cells. The treatments of these pathologies include radiotherapy, chemotherapy, as well as hormonal and immunomodulatory therapies. These conventional treatments may be inefficient as a result of the development of drug resistance (Hopfinger *et al*., 2012). In this sense, plants offer a wide variety of compounds that can be useful tools in the treatment of cancer.

Larrea divaricata Cavanilles (Zygophyllaceae) is an evergreen shrub that grows in South America. The leaves of *L. divaricata* are coated with a polyphenol-rich resin whose main compound is the nordihydroguaiaretic acid (NDGA) (Davicino *et al*., 2011). Although NDGA has antioxidant and antitumoral properties, evidences indicate that *L. divaricata* has other compounds with similar properties (Bongiovanni *et al*., 2008). Therefore, the searching for natural products other than NDGA is highly encouraged. A phytochemical analysis of an ethyl acetate fraction (EA) obtained from the aqueous extract of this plant was found to contain low levels of NDGA and high levels of flavonoids. Among flavonoids, quercetin-3-methyl ether (Q-3-ME) was identified as one of the compounds present in EA at a concentration of 0.52 g%. Both EA and Q-3-ME have been demonstrated to decrease the proliferation rate and viability of the EL-4 lymphoma cell line (Martino *et al*., 2013). However, the underlying mechanism by which these drugs exert their antiproliferative effect remains unknown.

Nitric oxide (NO) is a free radical derived from the metabolism of L-arginine through the action of nitric oxide synthases (NOS) (Luanpitpong and Chanvorachote, 2015). Works carried out over the past decades have demonstrated the capacity of NO to inhibit carcinogenesis and tumor growth in a concentration-dependent manner (Iyer *et al*., 2014).

The aim of this work was to elucidate the mechanism of action of the EA governing tumor inhibition, and to investigate the role of Q-3-ME in the biological activity observed for the whole fraction.

* Correspondence to: Renzo Martino, IQUIMEFA (UBA-CONICET), Junín 956 piso 2, 1113, Ciudad Autónoma de Buenos Aires, Buenos Aires, Argentina.
E-mail: renzo16martino@hotmail.com

Received 16 November 2015
Revised 01 March 2016
Accepted 03 March 2016

MATERIALS AND METHODS

Plant material. Leaves of *L. divaricata* Cav. were collected in the province of Córdoba, Argentina, and were identified by means of morphological, anatomical, and histochemical analyses. A voucher specimen was deposited at the Museum of Pharmacobotany, School of Pharmacy and Biochemistry, University of Buenos Aires (BAFC no. 38). The obtention of the EA fraction and the isolation of Q-3-ME were performed as described previously (Martino *et al*., 2013).

Cell line and culture conditions. The EL-4 lymphoma cell line (ATCC) is a murine T lymphocytic leukemia induced by the treatment of C57BL/6N mice with 9,10-dimethyl-1,2-benzanthracene. Cell suspensions from lymph nodes of C57BL/6N female mice (2–4 months old) were obtained aseptically by nylon wool purification of T cells as described previously (Martino *et al*., 2015). Resident macrophages were obtained from the peritoneal cavity, according to Martino *et al.* (2014). Animals were humanely handled according to the National Institutes of Health guide for the care and use of laboratory animals (NIH 8023, 1978). The protocols used in this work were approved by the Ethics Committee from the School of Pharmacy and Biochemistry, UBA (no. 220612-1).

The cells were cultured at optimal concentrations of 5×10^5 cells/ml in RPMI 1640 medium (Gibco, NY, USA) supplemented with 10% fetal calf serum (FCS, Internegocios, Argentina), 2 mM glutamine, and antibiotics (100 IU/ml penicillin and 100 μg/ml streptomycin) (Sigma, USA).

Apoptosis assays

Flow cytometry. To determine whether EA and Q-3-ME induced apoptosis in tumoral lymphocytes, the cells were incubated in the absence or the presence of different concentrations of EA or Q-3-ME for 6 h and 24 h. The cells were then washed and resuspended in binding buffer at a concentration of 1×10^6 cells. Aliquots of 1×10^5 cells were incubated with annexin V-FITC and propidium iodide (PI) for 15 min. The samples were diluted with binding buffer and analyzed by flow cytometry using a FACSCalibur flow cytometer (Becton Dickinson Biosciences). Data were analyzed with the Flow Jo 7.6 software, and expressed as the percentage of viable cells (annexin V−, PI−), early apoptotic cells (annexin V+, PI−), late apoptotic cells (annexin V+, PI+), and necrotic cells (annexin V−, PI+). In another set of experiments, the cells were incubated with the NOS inhibitor L-NG-nitroarginine methyl ester (L-NAME), before the addition of EA and Q-3-ME, and the percentage of annexin V-FITC positive cells was determined (Manuele *et al*., 2010).

Acridine orange–ethidium bromide staining. The presence of apoptotic morphology was determined by the acridine orange–ethidium bromide staining. Briefly, EL-4 cells were incubated for 6 h and 24 h at different concentrations of EA or Q-3-ME. The cells were then washed and resuspended in PBS. Ten microliters of a fluorescent dye mixture containing AO and EB (100 μg/ml) was added to the cells and incubated for 10 min. Freshly stained cell suspensions were dropped onto glass slides and covered by coverslips. The slides were observed under a UV-fluorescence microscope at a ×400 magnification (Di Rosso *et al*., 2013).

DNA fragmentation. To assess DNA fragmentation, EL-4 cells were lysed with lysis buffer (50 mM Tris-HCl pH 7.5; 1 mM EDTA; 0.2% Triton X 100), and centrifuged. The DNA was then precipitated with isopropanol and 5 M NaCl, and the samples were incubated overnight at −20 °C. The samples were then centrifuged, and the dry pellets were resuspended in loading buffer, resolved on a 1% agarose gel, and stained with ethidium bromide. The gels were then observed under UV light (Martino *et al*., 2012).

Mitochondrial membrane potential. EL-4 cells were cultured in the absence or presence of EA or Q-3-ME for 24 h, and then incubated with 1 μM rhodamine 123 for 30 min. The cells were then centrifuged and resuspended in PBS. Changes in the mitochondrial membrane potential were detected by flow cytometry using a FACSCalibur flow cytometer (Becton Dickinson Biosciences). Data were analyzed with the Flow Jo 7.6 software and expressed as the percentage of rhodamine 123 negative cells (Martino *et al*., 2015).

Western blot analysis. EL-4 cells were cultured in absence or presence of EA or Q-3-ME for different times. The cells were then lysed for 30 min at 4 °C in lysis buffer. After centrifugation (14 000*g*, 15 min, 4 °C), the whole-cell protein extracts (50 μg) were mixed with SDS sample buffer [2% SDS, 10% (v/v) glycerol, 62.5 mM Tris-HCl, pH 6.8, 0.2% bromophenol blue, and 1% (v/v) 2-mercaptoethanol]. Equal amounts of protein were separated by SDS-PAGE on 10% polyacrylamide gels, and transferred to PVDF membranes. Nonspecific binding sites on the PVDF membranes were blocked with blocking buffer (5% nonfat dried milk containing 0.1% Tween 20 in 100 mM Tris-HCl, pH 7.5, and 0.9% NaCl). The PVDF membranes were then incubated overnight with rabbit anti-active caspase 8, rabbit anti-active caspase 9, rabbit anti-active caspase 3, mouse anti-cleaved poly-(ADP-ribose)-polymerase (PARP), rabbit anti-iNOS, or rabbit anti-β-actin antibodies. All antibodies were used at a dilution of 1:1000 (Santa Cruz Biotech). After washing with PBS-Tween, the membranes were incubated with anti-rabbit or anti-mouse (1:2500) antibodies coupled to horseradish peroxidase for 1 h. After washing with PBS-Tween, an enhanced chemiluminescent system (ECL, GE Healthcare Life Sciences) was used for detection. A densitometric analysis of the bands was performed using Image J software (version 5.1, Silk Scientific Corporation, NIH, Bethesda, MA, USA). The intensities of the analyzed protein were normalized to those of the corresponding bands for β-actin (Di Rosso *et al*., 2013).

Total nitrite determination. The effect of EA and Q-3-ME on total nitrite production by EL-4 cells was determined using the Griess reagent. Briefly, the cells were incubated in the absence or presence of EA (100 μg/

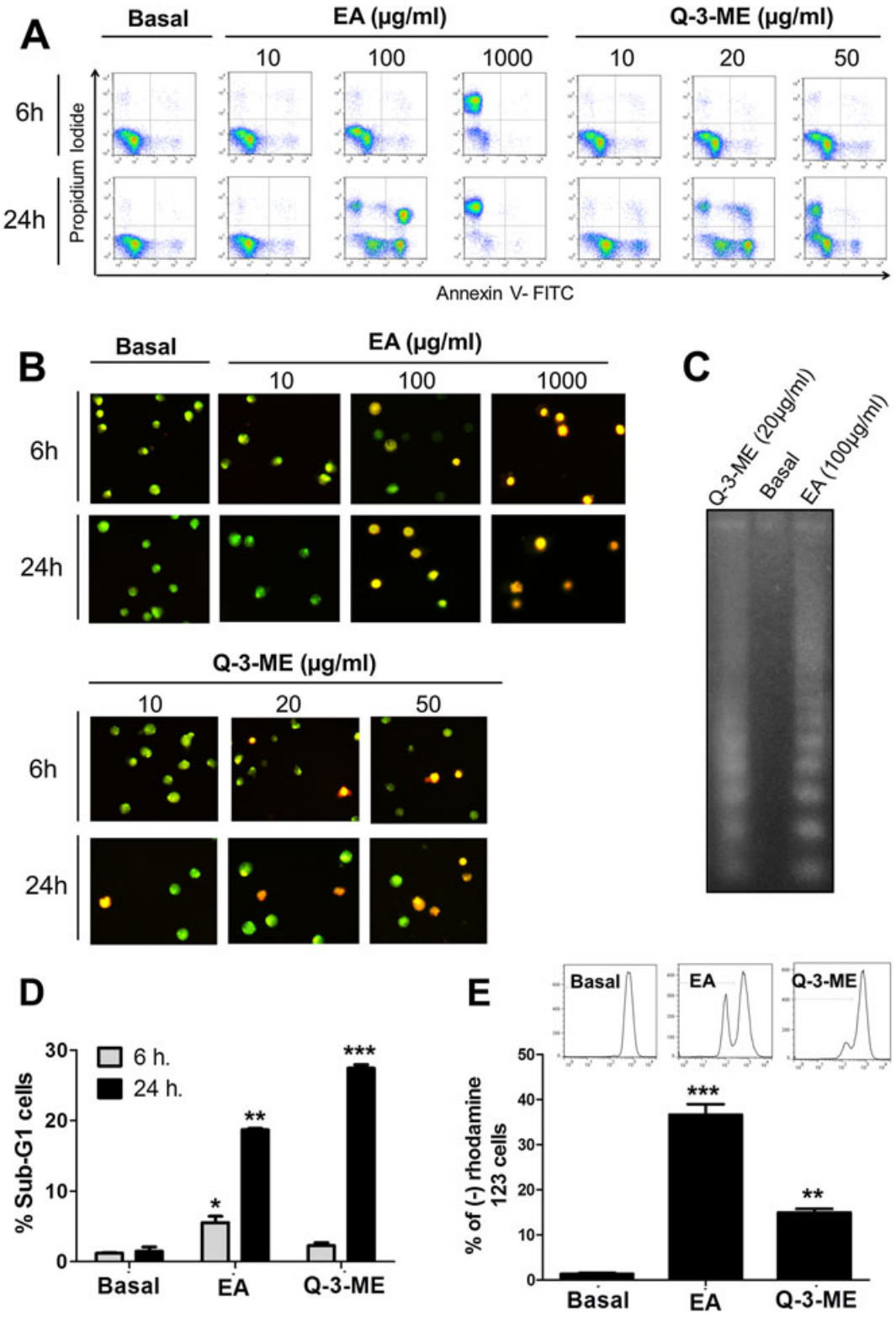

Figure 1. Apoptosis of EL-4 cells triggered by ethyl acetate (EA) and quercetin-3-methyl ether (Q-3-ME). (A) apoptosis evaluated by annexin V/PI staining. Cells were incubated with EA (10; 100 and 1000 µg/ml) or Q-3-ME (10, 20, and 50 µg/ml) for 6 h and 24 h. The cells were then analyzed by flow cytometry after incubation with annexin V-FITC and propidium iodide (PI). Graphs represent the dot plot analysis for each condition scored: viable cells (lower left quadrant, annexin V−/PI−), early apoptosis cells (lower right quadrant, annexin V+/ PI−), late apoptosis cells (upper right quadrant, annexin V+/PI+), and necrotic cells (upper left quadrant, annexin V−/PI+). (B) Apoptosis evaluated by acridine orange and ethidium bromide staining. After incubation with EA or Q-3-ME, EL-4 cells were labeled with acridine orange–ethidium bromide and analyzed by fluorescence microscopy (×400). The results are representative of three independent experiments. (C) DNA fragmentation assay. EL-4 cells were incubated with EA (100 µg/ml) or Q-3-ME (20 µg/ml) for 24 h. The DNA was precipitated, run in an agarose gel, and stained with ethidium bromide. The picture is representative of three independent experiments. (D) Effect of EA and Q-3-ME on DNA content. The cells were stained with PI, and the DNA content was determined by flow cytometry. The percentage of cells in the Sub-G1 phase was determined. The results represent the mean ± SEM of three independent experiments performed in triplicate. (E) Effect of EA and Q-3-ME on mitochondrial membrane potential. Changes in mitochondrial membrane potential were detected by flow cytometry. Histograms are representative of three independent experiments. The bar graph indicates the percentage of rhodamine 123negative cells. The results represent the mean ± SEM of three independent experiments performed in triplicate. $*p < 0.05$; $**p < 0.01$; $***p < 0.001$ significant differences with respect to basal conditions (ANOVA and Dunnett's test).

ml) or Q-3-ME (20 μg/ml) for 24 h. After incubation, culture supernatants were collected and centrifuged, and then incubated with the Griess reagent for 20 min in the dark, and measured at 540 nm. The concentration of total nitrites was derived from a standard curve (Martino *et al*., 2014).

Proliferation assessment. In order to establish a relationship between the induction of NO production and the inhibition of cell proliferation, the EL-4 cells were pre-incubated with the NOS inhibitor L-NAME, before EA or Q-3-ME stimulation. Cell proliferation was evaluated by the tritiated thymidine ([^{3}H]TdR) uptake technique, as described previously (Martino *et al*., 2013). The results were expressed as % of proliferation.

Determination of cell cycle arrest. Lymphoma cells were treated with EA (100 μg/ml) or Q-3-ME (20 μg/ml) for 3 h, 6 h, and 24 h. The untreated cells were used as control. After incubation, the cells were harvested and fixed with ice-cooled 70% ethanol at −20 °C for 2 h. Before the analysis, the cells were washed with cold PBS and resuspended in sodium citrate buffer, containing PI and RNase A. The DNA content was determined by a FACSCalibur flow cytometer (Becton Dickinson). The data were analyzed with the Flow Jo 7.6 software and expressed as percentage of cells in each stage (G0/G1, S, and G2/M). The percentage of cells in the Sub-G1 phase (nonviable cells) was determined (Martino *et al*., 2015).

Cell viability. The cell viability of normal lymphocytes and peritoneal macrophages was determined by the reduction of 3-(4,5-dimethylthiazol-2-yl)-2,5-diphenyltetrazolium bromide (MTT) as previously described (Martino *et al*., 2015). Briefly, the cells were incubated alone or in the presence of different concentrations of EA or Q-3-ME for 24 h. The MTT solution was then added and incubated for 4 h. The blue formazan formed was solubilized in acidic isopropanol. The absorbance was measured at 570 nm in a microplate reader. The untreated cells were used as 100 % viability control. The results were expressed as the percentage of viability relative to the control.

Statistics. The results are presented as mean ± SEM. The level of statistical significance was determined by a one-way analysis of variance (ANOVA) and the Dunnett's test. The GraphPad Prism 5.0 software (GraphPad Software Inc., San Diego, CA, USA) was employed. Comparisons were referred to the control group. P values <0.05 were considered significant.

RESULTS AND DISCUSSION

This study was aimed at elucidating the mechanism involved in the antiproliferative action of EA fraction from *L. divaricata* and its main flavonoid Q-3-ME on tumor cells.

EA fraction and Q-3-ME induce cell death through the intrinsic pathway of apoptosis

It is well known that drugs from plant origin can exert their antiproliferative activity by cytotoxic and/or cytostatic effects. A good example of both is vincristine, a cytostatic and cytotoxic alkaloid, with an IC_{50} value of 0.03 μg/ml in EL-4 cells. In this work, the mechanism by which EA fraction and its main flavonoid Q-3-ME exerted the previously reported antiproliferative activity was studied (Martino *et al*., 2013). In order to establish if these drugs have cytotoxic activity on EL-4 cells, apoptosis and/or necrosis phenomena were evaluated. To this end, the cells were treated either with EA or Q-3-ME at different concentrations and time. Fig. 1A and Table 1 show the percentage of viable cells and cells in different stages of apoptosis (early apoptosis, late

Table 1. Percentage of viable, early apoptotic, late apoptotic, and necrotic cells after 6 h and 24 h of culture with EA or Q-3-ME. Data represent the mean ± SEM

24 h	% viable	% early apoptosis	% late apoptosis	% necrosis
Basal	96.6 ± 0.4	2.5 ± 0.1	0.1 ± 0.0	0.8 ± 0.5
EA 10 μg/ml	96.5 ± 0.2	2.7 ± 0.1	0.3 ± 0.1	0.5 ± 0.1
EA 100 μg/ml	32.8 ± 2.7 **	25.1 ± 0.7 **	37.7 ± 1.2 ***	4.4 ± 0.8 *
EA 1000 μg/ml	4.9 ± 0.8 ***	0.9 ± 0.5	0.5 ± 0.5	93.7 ± 2.9 ***
Q-3-ME 10 μg/ml	85.4 ± 0.8 *	12.3 ± 1.0 *	1.4 ± 0.2 *	0.9 ± 0.1
Q-3-ME 20 μg/ml	36.3 ± 4.5 **	38.2 ± 0.9 **	6.6 ± 1.9 **	18.9 ± 5.5 *
Q-3-ME 50 μg/ml	50.4 ± 3.8 **	4.0 ± 0.2	0.9 ± 0.6	44.7 ± 3.4 **
6 h				
Basal	98.5 ± 0.2	0.6 ± 0.1	0.3 ± 0.1	0.6 ± 0.1
EA 10 μg/ml	96.8 ± 0.4	2.2 ± 0.1 *	0.4 ± 0.2	0.6 ± 0.3
EA 100 μg/ml	93.5 ± 1.1	5.0 ± 0.5 *	0.5 ± 0.1	1.0 ± 0.1
EA 1000 μg/ml	7.2 ± 2.4 ***	0.1 ± 0.1	0.1 ± 0.1	92.6 ± 4.5 ***
Q-3-ME 10 μg/ml	97.5 ± 1.4	1.6 ± 0.1	0.4 ± 0.1	0.5 ± 0.2
Q-3-ME 20 μg/ml	97.2 ± 2.5	1.8 ± 0.9	0.4 ± 0.2	0.6 ± 0.1
Q-3-ME 50 μg/ml	92.8 ± 0.8	6.1 ± 0.7 *	0.4 ± 0.1	0.7 ± 0.1

*$p < 0.05$.
**$p < 0.01$.
***$p < 0.001$.

apoptosis, and necrosis). The EA fraction (10 μg/ml and 100 μg/ml), as well as Q-3-ME (50 μg/ml), exerted their apoptotic effect (annexin V+/PI−) after 6 h of incubation. Interestingly, after 24 h of incubation, a concentration-dependent effect was observed when the cells were treated either with EA or Q-3-ME. A decrease in the percentage of viable cells and an increase in the percentage of the early and late apoptotic cells were observed with EA at 10 and 100 μg/ml and with Q-3-ME at 10 and 20 μg/ml. Finally, both EA and Q-3-ME induced necrosis at the highest concentrations tested (EA at 1000 μg/ml and Q-3-ME at 50 μg/ml). To corroborate these results, the cells were labeled with AO and EB, and analyzed by fluorescence microscopy (Fig. 1B). The control cells had green fluorescence and a nucleus with a normal morphology. Treatment with EA (100 μg/ml) for 6 h induced a change in the staining pattern, which turned the fluorescent green and orange, indicating the initiation of the apoptotic process. The number of apoptotic cells increased after 24 h. Furthermore, EA (1000 μg/ml) increased the number of cells with condensed nuclei and apoptotic bodies stained with fluorescent orange (6 h and 24 h), which is compatible with necrosis. In the case of Q-3-ME, the number of apoptotic cells increased in a time-dependent and concentration-dependent manner. Both EA (100 μg/ml) and Q-3-ME (20 μg/ml) induced the fragmentation of the DNA in internucleosomal fragments and a consequent increase in the number of cells in Sub-G1 phase. Taking these results together, we can conclude that the antiproliferative action of EA is due, at least in part, to the induction of apoptosis. These results are in line with those obtained by Davicino *et al*. (2010), who demonstrated that the *L. divaricata* aqueous extract was able to induce apoptosis in the BW5147 lymphoma cell line, in which increasing ROS and NO production, through a p38, ERK-1/2, and NF-κB pathways, were demonstrated. Q-3-ME was also found to induce apoptosis in EL-4 cells. This finding allows postulating Q-3-ME as one of the compounds responsible of the effects observed with EA.

Mitochondria plays an important role in the initiation and final stages of apoptosis. Several apoptotic insults induce mitochondrial membrane depolarization, which

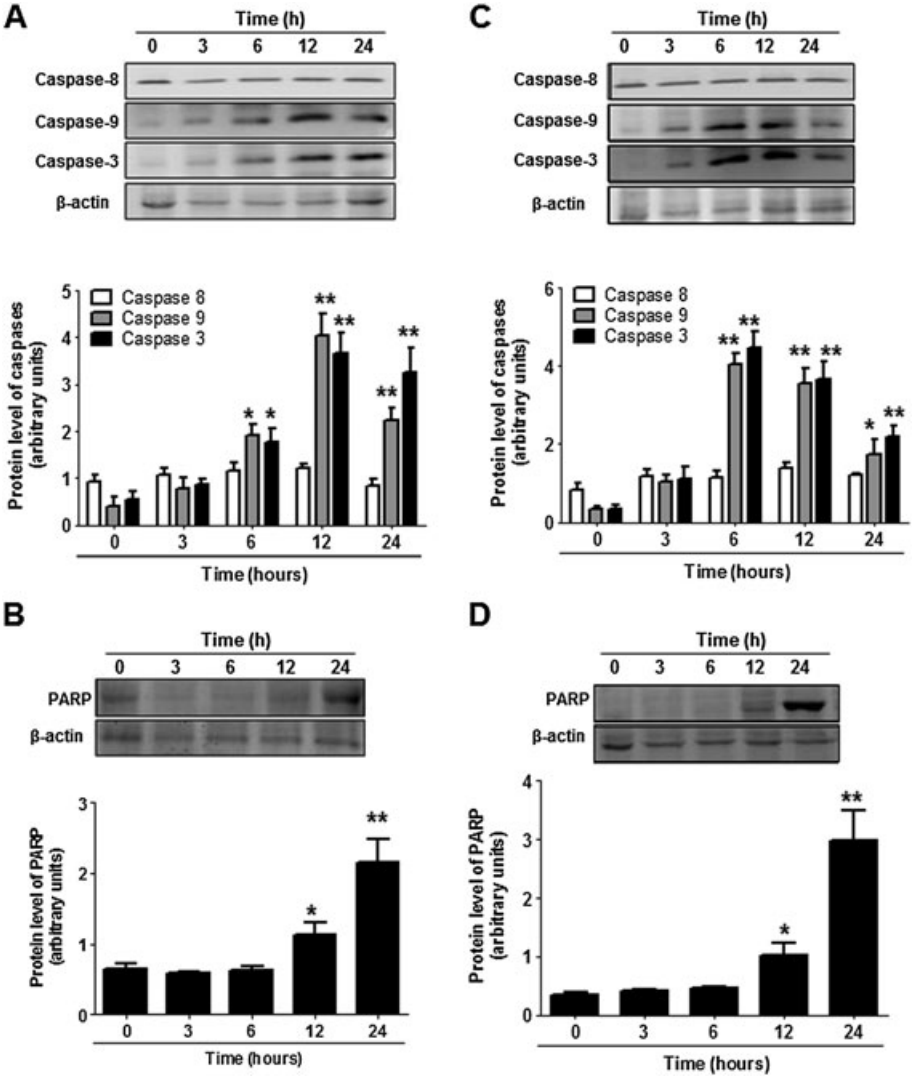

Figure 2. Caspases proteolytic activation and poly-(ADP-ribose)-polymerase (PARP) cleavage mediated by EA (A and C) and Q-3-ME (B and D). EL-4 cells were cultured in the absence (time 0 h) or presence of EA (100 μg/ml) or Q-3-ME (20 μg/ml) for the indicated times. Proteolytic activation of caspases 8, 9, and 3 and PARP cleavage were analyzed by western blot. Specific antibodies revealed bands for active caspase 8 (41 kDa), caspase 9 (37 kDa), active caspase 3 (17 kDa), cleaved PARP (89 kDa), and β-actin (43 kDa). Densitometric analyses are shown in the bar graphs. Values represent the mean ± SEM of three independent experiments. β-actin bands were used as loading control. $*p < 0.05$; $**p < 0.01$ significant differences with respect to basal conditions (ANOVA + Dunnett's test).

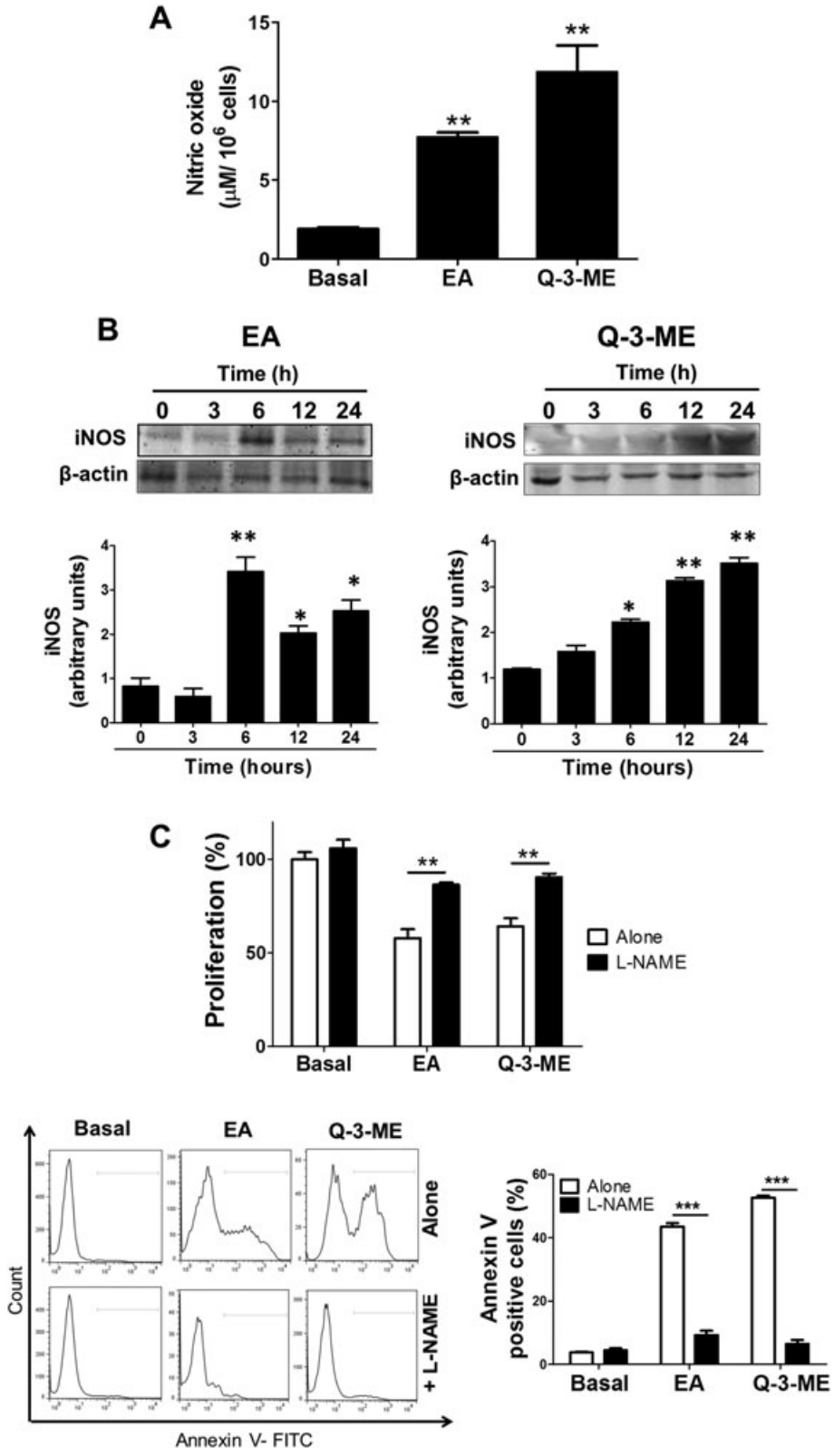

Figure 3. Role of nitric oxide (NO) in the antiproliferative effect of EA and Q-3-ME. (A) Production of NO by EL-4 cells. Tumor cells were incubated with EA (100 μg/ml) or Q-3-ME (20 μg/ml) for 24 h, and the NO produced was determined in culture supernatants. The results were expressed as μM of NO/10^6 cells, and represented the mean ± SEM of three independent experiments. (B) Inducible nitric oxide synthase expression (iNOS). The expression of iNOS (131 kDa) was determined by western blot analysis carried out with cells cultured for the indicated times. β-actin expression was used as loading control. Densitometric analyses were represented in the bar graphs as iNOS expression/β-actin expression. Values represent the mean ± SEM of three independent experiments. (C) Proliferation and apoptosis analysis. EL-4 cells were pre-incubated with L-NAME (a NOS inhibitor) before treatment with EA (100 μg/ml) or Q-3-ME (20 μg/ml) for 24 h. Cell proliferation was evaluated by the [^{3}H]TdR uptake, and expressed as % of proliferation relative to basal conditions. Apoptosis was evaluated by annexin V-FITC followed by flow cytometry analysis. Histograms and the bar graph indicate the percentage of annexin V positive cells. The results are expressed as the mean ± SEM of three independent experiments. $*p < 0.05$; $**p < 0.01$; $***p < 0.001$ significant differences respect to basal conditions (ANOVA + Dunnett's test).

is a consequence of the opening of the mitochondrial permeability transition pore. These membrane changes allow the release of apoptotic factors such as cytochrome c (Lopez and Tait, 2015). In order to understand the mechanism underlying the apoptotic activity of EA and Q-3-ME, their ability to interfere with the mitochondria membrane potential was evaluated by flow cytometry using rhodamine 123. As shown in Fig. 1E, both EA and Q-3-ME were able to decrease the mitochondrial membrane potential, as revealed by the presence of a significant increase in the number of rhodamine-123 negative cells ($p < 0.001$ for EA and $p < 0.01$ for Q-3-ME). These results indicate the initiation of a mitochondrial-dependent apoptotic process upon treatment with EA and Q-3-ME.

Upon release to the cytosol, cytochrome c binds to the adaptor molecule Apaf-1, and the activation of caspase-9 occurs through the formation of the apoptosome complex. Caspase-9 then activates caspase-3, which is the central caspase in the apoptotic signaling machinery. The latter signaling cascade is called 'intrinsic pathway of apoptosis' (Zaman *et al.*, 2014). Taking into account the involvement of mitochondria in cell death, the apoptosis pathway triggered by EA and Q-3-ME was also evaluated by western blot. As expected, EA (Fig. 2A) and Q-3-ME (Fig. 2C) were able to activate caspase-9 and caspase-3 as early as 6 h after stimulation, leading to an increase in the expression of the cleaved form of PARP after 12 h of incubation with the drugs (Figs. 2B and 2D). In fact, the highest levels of cleaved PARP were detected at the longest incubation time tested (24 h). This finding further supported the hypothesis indicating the requirement of sequential steps in the apoptotic event. On the other hand, no modifications in the levels of expression of cleaved caspase-8 were detected throughout the period of time tested. These results are in agreement with those obtained by Li *et al.* (2013), who have tested the activity of Q-3-ME on the breast cancer cell line SK-Br-3, demonstrating that this compound was able to induce apoptosis via caspase-3 and caspase-7 activation. When the EL-4 cells were treated with EA and Q-3-ME, the final stages of apoptosis were also observed. Such stages included chromatin condensation and DNA fragmentation (Fig. 1B, C, and D). Taking these results together, it can be concluded that EA and Q-3-ME exerted their cytotoxic effect through the activation of the intrinsic mitochondrial apoptotic pathway.

NO is involved in the antiproliferative action of EA and Q-3-ME

The role of NO and the nitrosative stress in the mechanism of action of EA and Q-3-ME was assessed. The treatment with EA or Q-3-ME significantly increased

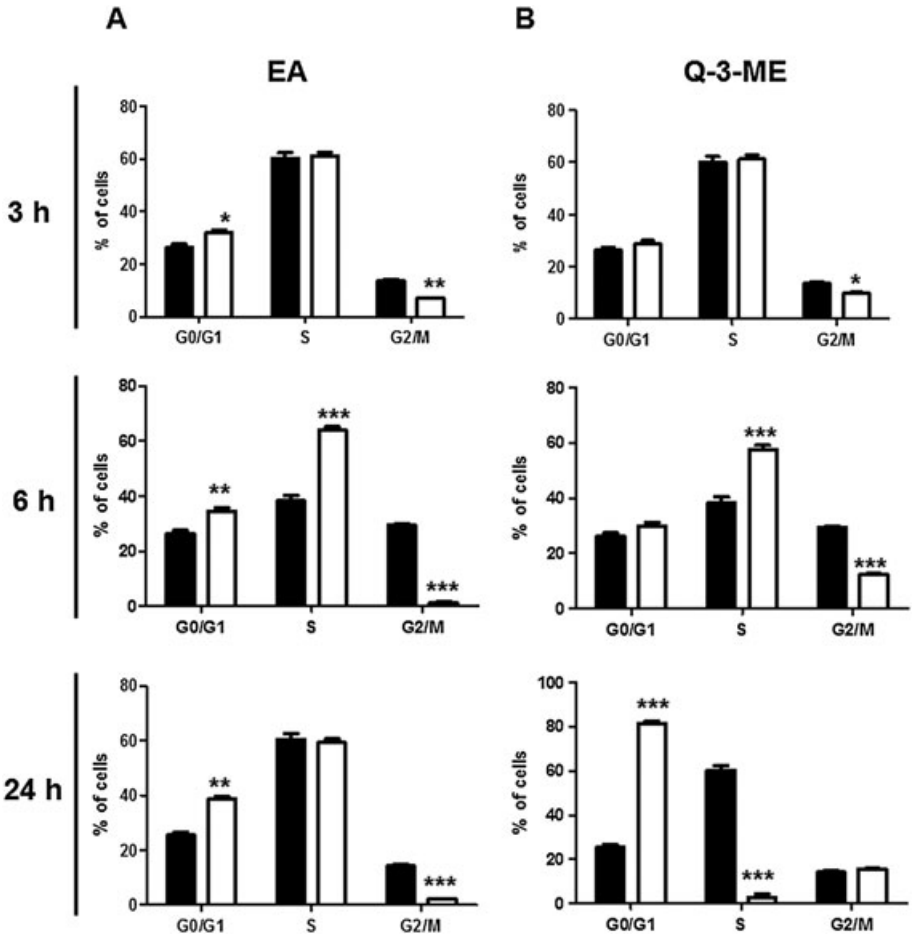

Figure 4. Effect of EA and Q-3-ME on the cell cycle of tumor cells. Cells were incubated with or without EA (100 μg/ml) (A) or Q-3-ME (20 μg/ml) (B) during 3 h, 6 h, and 24 h. After treatment, DNA was stained with PI and quantified by flow cytometry. Black bars represented untreated cells (basal), and white bars represent EA or Q-3-ME-treated cells. The results were expressed as % of cells in the different cell cycle phases (G0/G1; S and G2/M) and are expressed as the mean ± SEM of three independent experiments, performed in triplicate. $*p < 0.05$; $**p < 0.01$; $***p < 0.001$ significant differences with respect to basal conditions (ANOVA + Dunnett's test).

the NO production by EL-4 cells ($p < 0.01$) (Fig. 3A). These results are in line with the increased expression of iNOS found after the treatment of cells with EA or Q-3-ME. While Q-3-ME increased the expression of iNOS in a time-dependent manner, EA exerted the highest expression at 6 h of incubation (Fig. 3B). L-NAME was employed as a NOS inhibitor, and its effect on EL-4 cell proliferation and apoptosis was evaluated (Fig. 3C). The NO accumulation in tumor cells was responsible for the growth inhibition and apoptosis induction, because cells pre-incubated with L-NAME, before EA (100 μg/ml) or Q-3-ME (20 μg/ml) treatment, were able to revert the inhibition of proliferation exerted by both drugs ($p < 0.01$). A similar effect was observed when apoptosis was assessed: L-NAME was able to induce a significant decrease in the percentage of annexin-V positive cells (from 43.5% to 9.2% in the case of EA-treated cells and 52.7% to 6.5% in the case of Q-3-ME treatment; $p < 0.001$). It is known that NO can act as an intracellular messenger, as it can modulate various signaling pathways through nitration, S-nitrosylation, and DNA deamination, among others (Frederiksen *et al.*, 2007). NO has recently been demonstrated to have a great potential to inhibit carcinogenesis and tumor growth. Moreover, nitrosative stress can induce cell cycle arrest in the G0/G1 phase through the down regulation of the expression of cyclins D1 and E, and the up regulation of $p21^{waf1/cip1}$ expression in gastric cancer cells (Sang *et al.*, 2011). Therefore, NO could be the molecule responsible in EA and Q-3-ME cell cycle arrest. Other flavonoids, like fisetin, have been reported to have a similar mechanism of action in acute monocytic leukemia cells (Ash *et al.*, 2015).

Cytostatic effect of EA fraction and Q-3-ME

In order to investigate if EA and Q-3-ME have cytostatic activity, the effect on the cell cycle was analyzed. EA was able to arrest cells in G0/G1 phase as early as 3 h of cell culture, maintaining this state throughout the period of time evaluated. Q-3-ME exerted a strong, but slower effect than EA, by arresting almost 80% of the cells in the G0/G1 phase at 24 h. We also observed a decrease in the number of cells in the G2/M stage at all the timepoints tested (Fig. 4). These results indicate that although Q-3-ME is one of the compounds responsible of the cytostatic effect of EA, others might also be exerting a similar effect. Other authors have demonstrated that Q-3-ME can induce cell cycle arrest in SK-Br-3 breast cancer cells (Li *et al.*, 2013) and JB6 P+ epidermal cells (Li *et al.*, 2012). However, these authors observed an arrest in G2/M phase, suggesting that this flavonoid has probably a different impact on the proteins related to the cell cycle progression and arrest that are dependent on the cell line and the culture conditions employed.

Effect of EA and Q-3-ME on normal cell viability

Finally, the goal of any antitumoral treatment is to achieve a good selectivity, that is, a balance between efficacy and innocuousness (Machana *et al.*, 2012). In this sense, the viability of lymphocytes and macrophages was assessed by the MTT method. Neither EA nor Q-3-ME alone reduced MTT (data not shown). It was found that, at the concentrations that interfered with tumor cell proliferation, neither EA fraction nor Q-3-ME affected lymphocyte and macrophage viability (Fig. 5). Furthermore, the isolated flavonoid was capable of increasing macrophages MTT reduction at the highest concentrations tested ($p < 0.05$). The latter finding could be a result of a macrophage activation phenomenon. It

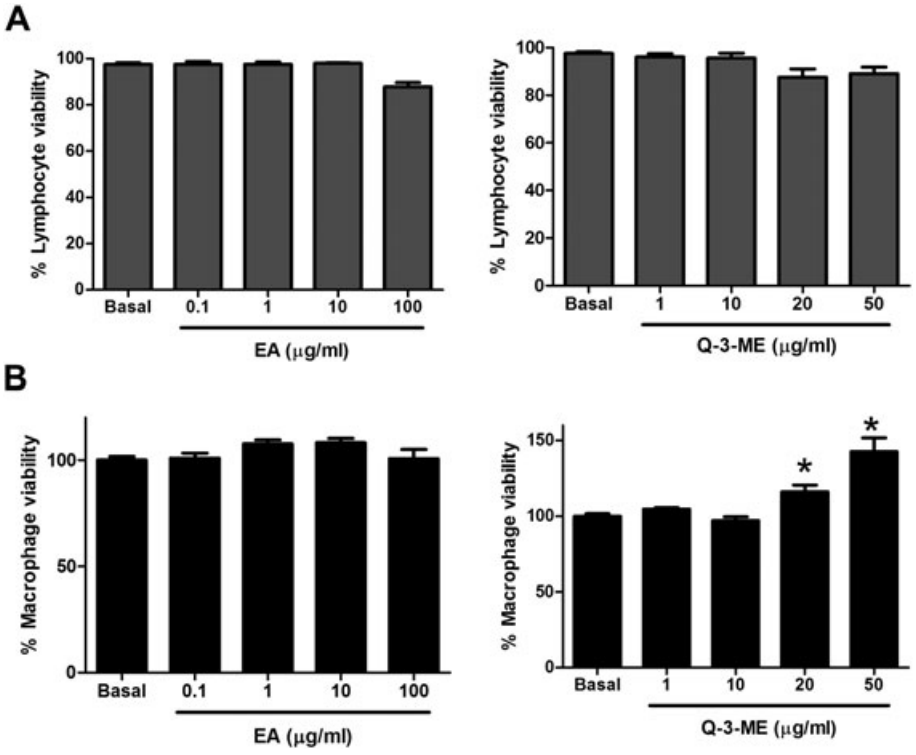

Figure 5. Effect of EA and Q-3-ME on normal lymphocyte and macrophage viability. Lymph nodes T lymphocytes (A) and peritoneal macrophages (B) from C57BL/6N mice were cultured with or without EA or Q-3-ME for 24 h. After that, cell viability was assessed by the MTT method. The results were expressed as cell viability (% of basal) and represent the mean ± SEM of three independent experiments $^*p < 0.05$ significant difference with respect to basal conditions (ANOVA + Dunnett's test).

is known that *L. divaricata* has immunomodulatory properties which are evidenced by the activation of macrophages by the classical pathway (Martino *et al*., 2014). This finding could be a helpful tool to enhance the immune system to eliminate cancerous cells *in vivo*.

CONCLUSIONS

The evaluation of the effectiveness of drugs against tumor lines and the analysis of the mechanisms of action involved could be useful in the search for novel therapeutic agents for cancer treatment. At the concentrations tested, EA and Q-3-ME proved to be active against lymphoma cells and nontoxic to normal cells. Furthermore, in this work, it was demonstrated that these drugs exerted their antiproliferative activity by inducing cell apoptosis by activation of the intrinsic pathway and by arresting the cell cycle in the G0/G1 phase. These effects seemed to be driven by NO. Taking into account the results obtained herein, EA and Q-3-ME could be considered good candidates to perform further studies to determine if they can be associated with other drugs used for cancer treatment.

Acknowledgements

This research was supported by PIP 0007 (Consejo Nacional de Investigaciones Científicas y Técnicas — CONICET, Argentina). Renzo Martino is a postdoctoral fellow of CONICET.

Conflict of Interest

The authors declare that they have no conflict of interest.

REFERENCES

Ash D, Subramanian M, Surolia A, Shaha C. 2015. Nitric oxide is the key mediator of death induced by fisetin in human acute monocytic leukemia cells. *Am J Cancer Res* **5**: 481–497.

Bongiovanni G, Cantero J, Eynard A, Goleniowski M. 2008. Organic extracts of *Larrea divaricata* Cav. induced apoptosis on tumoral MCF7 cells with a higher cytotoxicity than nordihydroguaiaretic acid or paclitaxel. *J Exp Ther Oncol* **7**: 1–7.

Davicino R, Manuele MG, Turner S, Ferraro G, Anesini C. 2010. Antiproliferative activity of *Larrea divaricata* Cav. on lymphoma cell line: participation of hydrogen peroxide in its action. *Cancer Invest* **28**: 13–22.

Davicino R, Martino R, Anesini C. 2011. *Larrea divaricata* Cav.: scientific evidence showing its beneficial effects and its wide potential application. *BLACPMA* **10**: 92–103.

Di Rosso M, Barreiro Arcos ML, Elingold I, *et al.* 2013. Novel o-naphthoquinones induce apoptosis of EL-4 T lymphoma cells through the increase of reactive oxygen species. *Toxicol In Vitro* **27**: 2094–2104.

Ferlay J, Soerjomataram I, Dikshit R, *et al.* 2015. Cancer incidence and mortality worldwide: sources, methods and major patterns in GLOBOCAN 2012. *Int J Cancer* **136**: E359–E386.

Frederiksen LJ, Sullivan R, Maxwell L, *et al.* 2007. Chemosensitization of cancer *in vitro* and *in vivo* by nitric oxide signaling. *Clin Cancer Res* **13**: 2199–2206.

Hopfinger G, Griessl R, Sifft E, *et al.* 2012. Novel treatment avenues for peripheral T-cell lymphomas. *Expert Opin Drug Discov* **7**: 1149–1163.

Iyer AK, Rojanasakul Y, Azad N. 2014. Nitric oxide and aggressive behavior of lung cancer cells. *Nitric Oxide* **42**: 9–18.

Li J, MottamalM LH, Liu K, *et al.* 2012. Quercetin-3-methyl ether suppresses proliferation of mouse epidermal JB6 P+ cells by targeting ERKs. *Carcinogenesis* **33**: 459–465.

Li J, Zhu F, Lubet R, *et al.* 2013. Quercetin-3-methyl ether inhibits lapatinib-sensitive and resistant breast cancer cell growth by inducing G2/M arrest and apoptosis. *Mol Carcinog* **52**: 134–143.

Lopez J, Tait SW. 2015. Mitochondrial apoptosis: killing cancer using the enemy within. *Br J Cancer* **112**: 957–962.

Luanpitpong S, Chanvorachote P. 2015. Nitric oxide and aggressive behavior of lung cancer cells. *Anticancer Res* **35**: 4585–4592.

Machana S, Weerapreeyakul N, Barusrux S. 2012. Anticancer effect of the extracts from *Polyalthia evecta* against human hepatoma cell line (HepG2). *Asian Pac J Trop Biomed* **2**: 368–374.

Manuele MG, Barreiro Arcos ML, Davicino R, Ferraro G, Cremaschi G, Anesini C. 2010. Limonene exerts antiproliferative effects and increases nitric oxide levels on a lymphoma cell line by dual mechanism of the ERK pathway: relationship with oxidative stress. *Cancer Invest* **28**: 135–145.

Martino R, Davicino R, Mattar MA, *et al.* 2012. Macrophages activation by a purified fraction, free of nordihydroguaiaretic acid (NDGA), from *Larrea divaricata* Cav. as a potential novel therapy against *Candida albicans*. *Immunopharmacol Immunotoxicol* **34**: 975–982.

Martino R, Sülsen V, Alonso R, Anesini C. 2013. A fraction rich in phenyl propanoids from *L. divaricata* aqueous extract is capable of inducing apoptosis, in relation to H_2O_2 modulation, on a murine lymphoma cell line. *Leukemia Res* **37**: 1137–1143.

Martino R, Canale F, Sülsen V, *et al.* 2014. A fraction containing kaempferol-3,4 -dimethylether from *Larrea divaricata* Cav. induces macrophage activation on mice infected with *Candida albicans*. *Phytother Res* **28**: 917–924.

Martino R, Beer MF, Elso O, Donadel O, Sülsen V, Anesini C. 2015. Sesquiterpene lactones from *Ambrosia* spp. are active against a murine lymphoma cell line by inducing apoptosis and cell cycle arrest. *Toxicol In Vitro* **29**: 1529–1536.

Sang J, Chen Y, Tao Y. 2011. Nitric oxide inhibits gastric cancer cell growth through the modulation of the Akt pathway. *Mol Med Rep* **4**: 1163–1167.

Zaman S, Wang R, Gandhi V. 2014. Targeting the apoptosis pathway in hematologic malignancies. *Leuk Lymphoma* **55**: 1980–1992.

